

Optical Analysis of Hg^{2+} Ions by Oligonucleotide–Gold-Nanoparticle Hybrids and DNA-Based Machines**

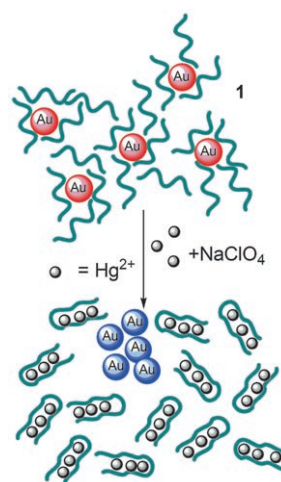
Di Li, Agnieszka Wieckowska, and Itamar Willner*

Mercury ions act as severe environmental pollutants and they have serious medical effects.^[1] Specifically, microbial biomethylation of mercuric ions (Hg^{2+}) yields methyl mercury that accumulates in the body through the food chain, and is known to cause brain damage and other chronic diseases.^[2] Also, it is important to control the leakage of Hg^{2+} ions from amalgam fillings in teeth during dental care.^[3] Hence, the rapid and sensitive analysis of Hg^{2+} ions in water or food resources is important,^[4] and the analysis of Hg^{2+} ions in human fluids, for example, saliva has considerable diagnostic value. Different procedures for the analysis of Hg^{2+} ions were developed, including electrochemical methods,^[5] optical methods that include Hg^{2+} -sensitive fluorophores or chromophores,^[6] and the use of proteins^[7] and functional polymer materials.^[8] Metal nanoparticles and semiconductor quantum dots^[9] have been applied for the analysis of Hg^{2+} ions. The complexation of metal ions with nucleotide purine and pyrimidine bases attracted recent research efforts,^[10] and the formation of Hg^{2+} -bis-thymine complexes^[11] is well established. Indeed, various Hg^{2+} ion detection assays based on the Hg^{2+} -thymine complexes in DNA were developed in the recent years. Thymine (T)-rich nucleic acids separated by a spacer and tethered at their ends with fluorophore/quencher units were used to analyze Hg^{2+} ions by the ion-induced formation of a hairpin structure that yields an intramolecular fluorescence resonance energy transfer (FRET) process.^[12] The interaction of conjugated polymers with T-rich nucleic acids that are self-organized in the form of a hairpin structure by Hg^{2+} ions led to the fluorescence detection of Hg^{2+} ions by the respective polymer–DNA complexes.^[13] Poly-T-functionalized gold nanoparticles (AuNPs) were aggregated with single-T-mutant-functionalized AuNPs in the presence of polyadenine (poly-A). The melting temperature of the resulting aggregate, and as a result, the red-to-blue optical transition, were found to be controlled by the concentration of Hg^{2+} ions; the presence of the Hg^{2+} ions causes a the formation of interparticle T-Hg²⁺-T complexes.^[14] Recently, the allosteric

Hg^{2+} -induced activation of a UO_2^{2+} -ion-dependent DNAzyme was used for the amplified detection of Hg^{2+} by fluorescence.^[15] Herein we describe two different optical methods to analyze Hg^{2+} ions that are based on the formation of a Hg^{2+} -bis-thymine complex. These methods are: 1) The analysis of Hg^{2+} using aggregated AuNPs; 2) The analysis of Hg^{2+} ions using a DNA-based machine.

Single-stranded nucleic acids were found to interact with AuNPs, resulting in the uncoiling of the oligonucleotides and the association of the nucleotide bases to the NPs. This stabilizes the NPs against aggregation under high ionic strength conditions.^[16]

The formation of double-stranded DNA,^[17] or the generation of oligonucleotide–protein complexes,^[18] were found to desorb the single-stranded nucleic acids from the AuNPs, thus inducing the aggregation of the NPs. This aggregation resulted in a red-to-blue color change owing to the interparticle coupled plasmon excitons in the aggregated states.^[19] This property was employed to develop DNA or protein AuNP-based sensors. Scheme 1 depicts the method to analyze



Scheme 1. Hg^{2+} -ion-stimulated aggregation of AuNPs for the optical analysis of Hg^{2+} ions.

Hg^{2+} ions through the aggregation of AuNPs. AuNPs (13 nm, 5 nm) were treated with the nucleic acid (**1**; 100 nM), then NaClO_4 (100 mM) was added to the NPs solution. Under these conditions, the mixture of NPs is stable even in the presence of the added salt. The nucleic acid **1** includes two T-rich domains spaced by a “mute” oligonucleotide sequence. The complexation of Hg^{2+} with the T sites of **1** yields a hairpin complex, the formation of which removes **1** from the AuNPs. In the presence of the destabilizing salt, the NPs undergo

[*] Dr. D. Li,^[†] Dr. A. Wieckowska,^[†] Prof. I. Willner
Institute of Chemistry
The Hebrew University of Jerusalem
Jerusalem 91904 (Israel)
Fax: (+972) 2-6527-715
E-mail: willnea@vms.huji.ac.il

[†] These authors contributed equally to this work.

[**] This research is supported by the EC VSN project. We thank Mr. Roni Nowarski and Dr. Xiaomeng Sui for their assistance in the gel electrophoresis and TEM experiments.

Supporting information for this article is available on the WWW under <http://www.angewandte.org> or from the author.

aggregation, resulting in a color change. It should be noted that NaClO₄ was selected as ionic-strength destabilizer of the NP system because other anions, such as Cl[−], SO₄^{2−}, or PO₄^{3−}, form an insoluble product with Hg²⁺ ions, a process that breaks the association of the Hg²⁺ ions with the T-bases.

5'-TTCTTTCTCCCTTGTTTGGT-3' (1)

5'-CCAACCCCCAGAAAGAA-3' (2)

Figure 1(A), curves (a)–(f), show the absorbance spectra of the 1/AuNP system with different concentrations of Hg²⁺ ions for a fixed time of 20 min. At higher concentrations of Hg²⁺ ions, the red-shifted band corresponding to the aggregated NPs is intensified, and this is accompanied by a decrease in the plasmon absorbance of the individual AuNPs. These results are consistent with a higher degree of aggregation upon addition of Hg²⁺ ions. The resulting blue color originates from the Hg²⁺-ion-induced aggregation of the NPs that yields an interparticle coupled plasmon absorbance. Figure 1(A), inset, depicts the calibration curve that corresponds to the absorbance changes of the system at different concentrations of Hg²⁺ ions. The method enables the analysis of Hg²⁺ ions with a limit of determination that corresponds to 10 nm (2 ppb). The aggregation of the AuNP in the presence of Hg²⁺ ions is attributed to the formation of a rigid hairpin structure in which the T residues of the spatially separated nucleotides are linked by the Hg²⁺ ions. The stiff structure of the Hg²⁺-bridged nucleic acids, similarly to duplex DNA, cannot wrap around and stabilize the AuNPs, leading to their aggregation in the high ionic-strength medium. AuNPs stabilized by a DNA sequence without T residues (2), however, do not aggregate in the presence of Hg²⁺ ions and salt (Figure 1(A), curve (g)). The Hg²⁺-ion-stimulated aggregation of the AuNPs is further supported by TEM images [Figure 1(B), image (a)] that reveal individual nanoparticles in the absence of Hg²⁺ ions and aggregation of NPs in the presence of Hg²⁺ ions [Figure 1(B), image (b)]. The visual detection of the presence of Hg²⁺ ions is also possible. Figure 1(C) shows the color changes of the 1/AuNP solution upon treatment with Hg²⁺ ions.

The 1/AuNP system is selective for Hg²⁺ ions. Figure 2 depicts the absorbance changes for the 1/AuNP system upon interaction with different metal ions. These changes are minute with all the other metal ions (10 μM) except Pb²⁺. The interference of Pb²⁺ ions is masked upon the use of 2,6-pyridinedicarboxylic acid (pdca) as a co-additive. This procedure leads to a AuNPs system insensitive towards aggregation induced by Pb²⁺-ions,^[20] whereas the analysis of Hg²⁺ ions is almost unaffected in the presence of the pdca ligand. These results imply that the Hg²⁺-ion-induced aggregation of AuNPs stabilized by 1 is selective and provides a visual rapid test for the sensitive detection of Hg²⁺ ions. Furthermore, it should be noted that this selectivity pattern is retained even at lower concentrations of the Hg²⁺ ions (see Supporting Information, Figure S1). Also, Hg²⁺ ions can be easily analyzed with a signal-to-noise ratio (S/N) of 3 at a concentration of 1 × 10^{−7} M when all the other metal ions are present at a 100-fold higher concentration.

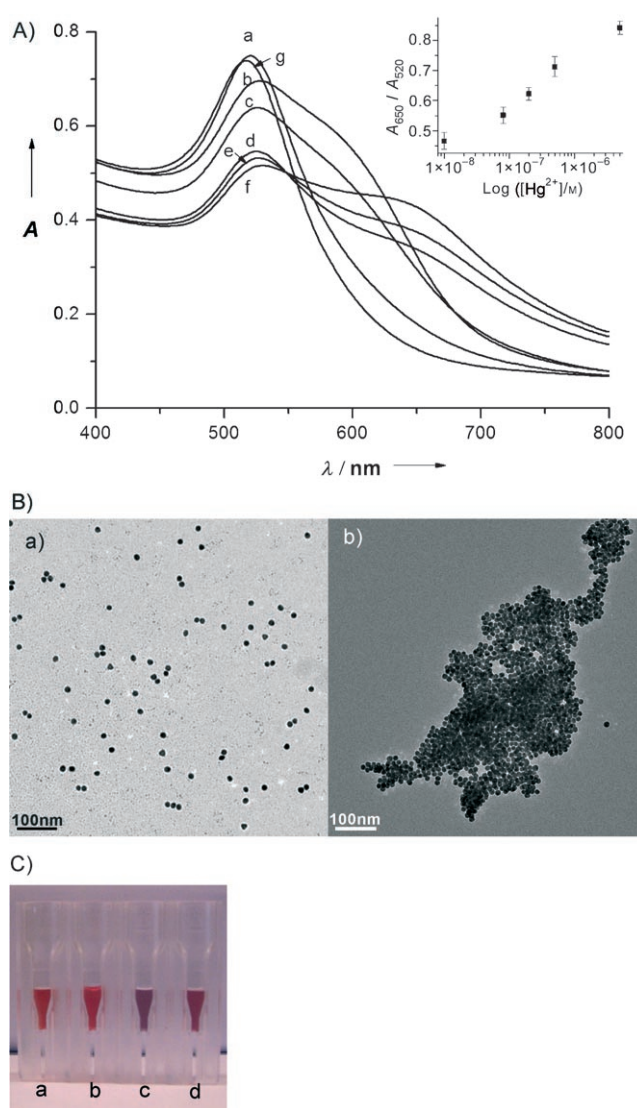


Figure 1. A) Absorption spectra corresponding to the analysis of different concentrations of Hg²⁺ ions in the presence of the 1/AuNPs system containing NaClO₄ (100 mM): a) 0 M, b) 1 × 10^{−8} M, c) 8 × 10^{−8} M, d) 2 × 10^{−7} M, e) 5 × 10^{−7} M, f) 5 × 10^{−6} M, g) The AuNP stabilized by the foreign (T-lacking) nucleic acid 2, in the presence of Hg²⁺ ions (5 × 10^{−6} M). Inset: Derived calibration curve. All experiments were recorded in NaClO₄ (100 mM) solution. B) TEM images of a) the non-aggregated AuNPs stabilized by 1 in the presence of NaClO₄ (100 mM), b) the aggregated AuNPs after treatment of the 1/AuNPs system with Hg²⁺ (5 × 10^{−6} M) in the presence of NaClO₄ (100 mM). C) Visual color changes upon treatment of the DNA/AuNPs system with different concentrations of Hg²⁺ ions in the presence of NaClO₄ (100 mM). a) 1/AuNPs, b) 2/AuNPs in the presence of Hg²⁺ (5 × 10^{−6} M), c) 1/AuNPs in the presence of Hg²⁺ (1 × 10^{−7} M), d) 1/AuNPs in the presence of Hg²⁺ (5 × 10^{−8} M).

The use of DNA-based machines as molecular systems for amplified biosensing has attracted substantial recent research efforts.^[21] In this approach, a tailored nucleic acid acts as a “track” for the recognition and operation of the machine. Upon binding of the analyte to the track, and in the presence of the appropriate “fuel substrate”, the autonomous operation of the machine functions on the track are triggered. Machine-like operations included, replication, scission, and

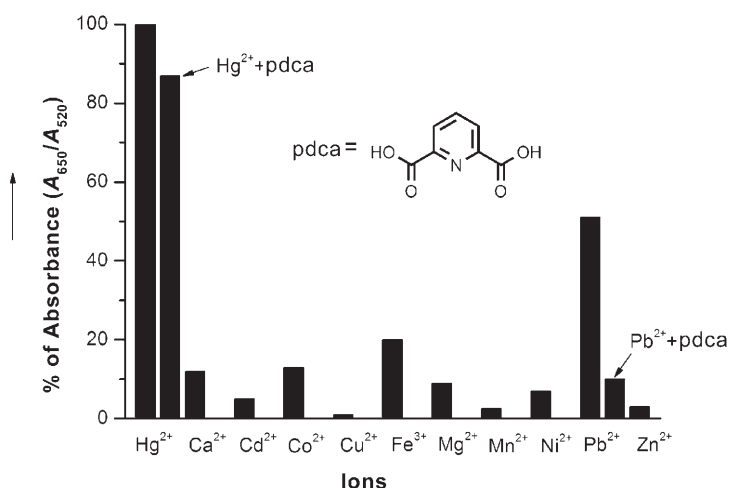


Figure 2. Selectivity of the analysis of Hg^{2+} ions by the method depicted in Scheme 1. The concentration of all the metal ions was $10 \mu\text{M}$.

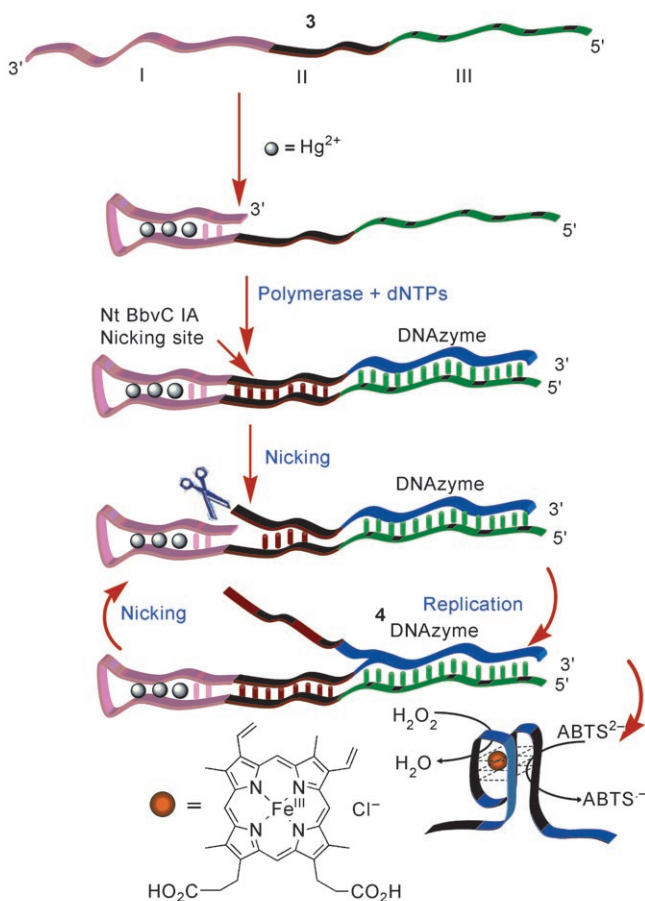
displacement processes. The DNA strand displaced from the track acts as the “product” of the machine. By appropriate tailoring of the product to act as a DNAzyme or to generate

fluorescence, it could be used as a transducing element to provide a “read out” of the operation of the machine, and for the primary detection of the respective analyte. Indeed, DNA-based machines were used to detect DNA^[22a] and to analyze low-molecular-weight substrates (for example, cocaine).^[22b] This approach was further extended to analyze Hg^{2+} ions (Scheme 2). The nucleic acid track, **3**, includes three regions. Domain I includes the Hg^{2+} -ion recognition sequence that is composed of two T-rich regions separated by a spacer of random bases. The domain II represents the “heart” of the molecular machine, and upon its replication, the complementary strand includes the specific sequence for nicking by Nt BbvC 1A. Domain III includes the sequence that is complementary to the horseradish peroxidase (HRP)-mimicking DNAzyme.^[23] In the presence of Hg^{2+} ions the nucleic acid sequence I folds into a hairpin structure, where the 3'-end hybridizes with a complementary part of

the track. Formation of the duplex region initiates, in the presence of polymerase/dNTPs, the replication of the track. The replicated strand in the region II of the track includes the sequence-specific nicking site for Nt BbvC 1A. The cleavage of the site results in the initiation of a secondary polymerization cycle while displacing the sequence, **4**, that self-assembles into the G-quadruplex-hemin DNAzyme structure that mimics the horseradish peroxidase. This catalyzes the oxidation of 2,2'-azino-bis(3-ethylbenzothiazoline-6-sulfonic acid) diammonium salt (ABTS^{2-}) by H_2O_2 to the colored product, $\text{ABTS}^{\cdot-}$. Thus, the recognition of the Hg^{2+} ions triggers the autonomous operation of the machine that synthesizes the DNAzyme. The repeated synthesis of the DNAzyme and its catalytic activity lead to a two-step amplification of the sensing process.

5'-CCCAACCCGCCCTACCCGCTGAGGTTCCCCAGATTC-
TTTCTTCCCTTGTGTTTCTGGGG-3' (**3**)

5'-CAGCGGGTAGGGCGGGTTGGG-3' (**4**)



Scheme 2. The analysis of Hg^{2+} ions by a DNA-based machine utilizing **3** as a track, and the autonomous synthesis of the HRP-mimicking DNAzyme units by repeated replication/nicking cycles, see text for details.

Figure 3 shows the absorbance changes observed upon activation of the DNA machine by different concentrations of Hg^{2+} ions. As the concentration of Hg^{2+} ions increases, more “DNA tracks” are activated for the synthesis of the DNAzyme, and the generation of the colored product is intensified. The absorbance changes observed in the absence of Hg^{2+} ions are attributed to the minute folding of **3** to the duplex structure. The folded structure activates the replication/nicking machine that yields, inefficiently, the DNAzyme units. These units catalyze, in the presence of hemin, the oxidation of ABTS^{2-} by H_2O_2 . The oxidation rate of ABTS^{2-} in the absence of the track **3** and in the presence of hemin only is depicted in Figure 3 f. The method enabled the analysis of Hg^{2+} ions with a sensitivity limit that corresponds to 1 nM (0.2 ppb). The detection of ions by the DNA track **3** is selective for Hg^{2+} (Figure 4). Treating **3** with different metal ions, polymerase/dNTPs, and Nt BbvC 1A, results in changes in the ABTS^{2-} absorbance similar to those observed with

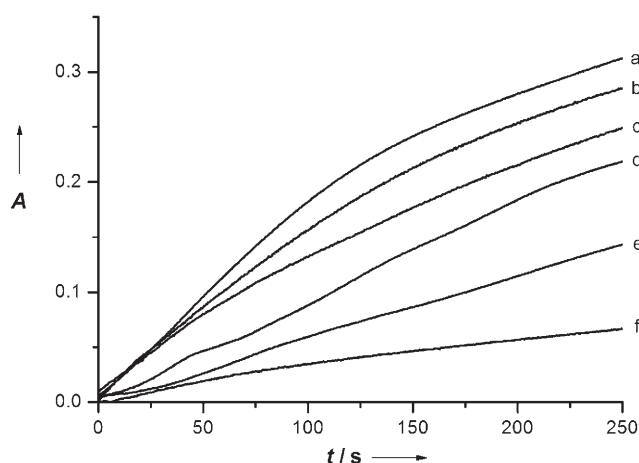


Figure 3. Time-dependent absorbance changes upon analyzing different concentrations of Hg^{2+} ions by the DNA-based-machine approach depicted in Scheme 2: a) 5×10^{-7} M, b) 1×10^{-7} M, c) 1×10^{-8} M, d) 1×10^{-9} M, e) 0 M. f) the spectral changes induced only by hemin (1×10^{-7} M). In experiments shown in (a)–(e), the system included: **3** (5×10^{-8} M), dNTPs (0.1 mM), polymerase (10 units), Nt BbvC 1A (20 units) in a combination of NEB buffer 4 and MOPS buffer solution, pH 7.9 (for composition, see Experimental Section). After the synthesis of the DNazymes, hemin (1×10^{-7} M), H_2O_2 (2 mM), and ABTS^{2-} (2 mM) were added to the system, and the absorption spectra were recorded.

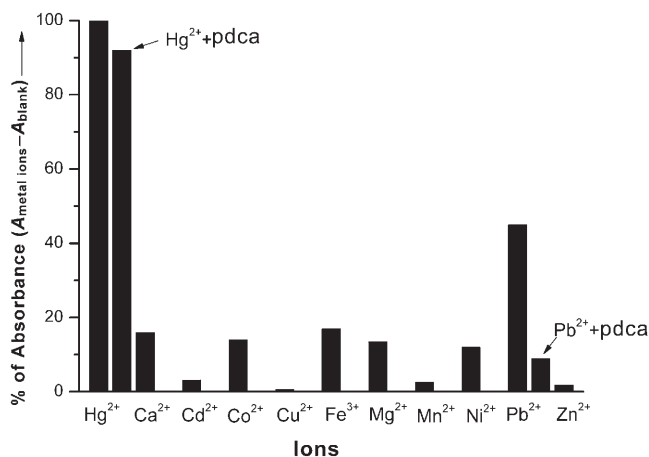


Figure 4. Selectivity study corresponding to the analysis of Hg^{2+} by the DNA machine described in Scheme 2. The concentration of all the metal ions was 10 μM .

hemin only (background absorbance). Only Pb^{2+} ions (10 μM), generated an interfering absorbance; this corresponded to 50% of the signal for Hg^{2+} ions. The effect of this interfering ion was removed, however, by the addition of pdca; this masked the Pb^{2+} ions, yet had only a minute effect on the absorbance changes generated by Hg^{2+} ions ($< 8\%$). It should be noted that the selectivity pattern is retained even at low concentrations of Hg^{2+} ions (see Supporting Information, Figure S2). Furthermore, the signal of the interfering ions is not linear with the concentration, and it remains at a low value, even at high concentrations of the ion. For example, we

analyzed 1×10^{-7} M Hg^{2+} ion with the DNA machine, and compared the resulting absorbance to that generated by a 1000-fold higher concentration of Ca^{2+} ions. The absorbance signal of the Hg^{2+} ions is still three-time higher than that of the Ca^{2+} ions (see supporting information, Figure S3).

The formation of the displaced DNzyme units upon the Hg^{2+} -induced activation of the machine was further supported by gel electrophoresis experiments, (See Supporting Information, Figure S1). In the presence of Hg^{2+} ions, the appearance of a new nucleic acid band at the molecular weight corresponding to the displaced oligonucleotide was observed. The respective band of the DNzyme sequence intensified when the concentration of Hg^{2+} ions was higher.

To conclude, the present study has introduced two methods for the optical analysis of Hg^{2+} ions by nucleic acid assays. The first method is based on the Hg^{2+} -ion-induced aggregation of AuNPs that were stabilized by the nucleic acid units which can bind Hg^{2+} ions. The method reveals a sensitivity that corresponds to 10 nM (2 ppb). Albeit the sensitivity of this method is only slightly improved as compared to other Hg^{2+} -ion detection schemes,^[11] the simplicity of the method and the qualitative visual imaging of the presence of Hg^{2+} ions at low concentrations, however, make the system an attractive analytical tool. The second method involved the colorimetric detection of Hg^{2+} ions by a DNA-based machine. This method involves two amplification steps, and its advantage is highlighted by the unprecedented sensitivity that corresponds to 1 nM (0.2 ppb). This method reveals a substantial enhancement in the sensitivity over the reported methods, and comparable sensitivity to the recently reported DNzyme method.^[15] However, as the DNzyme method requires the labeling of the system with donor–acceptor labels, we feel that our method demonstrates analytical advantages. It should be noted that the present procedures analyze Hg^{2+} ions in pure aqueous solutions, and the results are compared to related analytical methods that addressed the determination of Hg^{2+} ions in pure aqueous environmental samples. The analysis of Hg^{2+} in real biological fluids or environmental samples will certainly face the interference of other components and thus, the determination limits for Hg^{2+} ion will need to be further evaluated. Preliminary experiments were performed on contaminated underground water that includes 40 ppb of Hg^{2+} ions. The results revealed clear difference between pure underground water and the contaminated sample. (see Supporting Information).

Experimental Section

Materials: HAuCl_4 , $\text{Hg}(\text{ClO}_4)_2$, and sodium citrate were purchased from Aldrich and used as received. Oligonucleotides **1–4** were synthesized by Sigma Genosys. The deoxynucleotide solution mixture, dNTPs, in NEB buffer 4, Tris-acetate (20 mM), MgAc (10 mM), KAc (50 mM), dithiothreitol (DTT; 1 μM), pH 7.9, the Nt BbvC 1A endonuclease (New England BioLabs), and polymerase Klenow fragment *exo-* (Amersham Biosciences), hemin (Frontier Scientific) were used without any further purification.

Preparation of AuNPs: Gold nanoparticles with an average diameter of 13 nm were prepared using the citrate reduction method. Briefly, a solution of sodium citrate (10 mL; 38 mM) was added to a

rapidly stirred boiling aqueous solution of HAuCl_4 (100 mL; 1 mM). After 10 more minutes of boiling, the solution was allowed to cool to room temperature, and the AuNPs were collected by filtering through a 0.8 μm membrane.

The optical detection of Hg^{2+} using AuNPs: DNA **1** (100 nM) 2-[4-(2-hydroxyethyl)-1-piperazinyl]ethanesulfonic acid (HEPES; 10 mM, pH 7.4) was mixed with AuNPs (5 nM) for 15 min. The resulting solution was mixed with different concentrations of Hg^{2+} ions. The mixture was allowed to react for 20 min and then salt solution (NaClO_4 ; 100 mM) was added.

Operation of the DNA machine: Different concentrations of Hg^{2+} ions were incubated with DNA **3** (50 nM), for 15 min in a buffer solution (Tris-acetate (20 mM), 3-(4-morpholinyl)-1-propanesulfonic acid (MOPS; 10 mM), NaNO_3 (50 mM), MgAc (10 mM), KAc (50 mM), DTT (1 μM), pH 7.9). Then the machine was operated by adding polymerase (10 units), Nt BbvC 1 A (20 units), and dNTPs (0.1 mM) to the mixture and incubating at 37°C for 1 h. The machine was then stopped by cooling to 4°C for further colorimetric measurements.

Colorimetric Measurements Assay: The experiment was performed in a solution consisting of the products, hemin (10^{-7}M), H_2O_2 (2 mM), 2,2'-azino-bis(3-ethylbenzothiazoline-6-sulfonic acid) diammonium salt (ABTS^{2-} ; 2 mM), in a buffer solution consisting of Tris-acetate (20 mM), MOPS (10 mM), KAc (50 mM), NaNO_3 (50 mM), MgAc (10 mM), DTT (1 μM), pH 7.9, 25°C. Absorbance changes at 415 nm were monitored to characterize the rate of oxidation of ABTS^{2-} .

Received: December 30, 2007

Published online: April 11, 2008

Keywords: analytical methods · DNA machines · gold · mercury · nanoparticles

- [1] a) W. H. Organization, *Environmental Health Criteria 118: Inorganic Mercury*, World Health Organization, Geneva, **1991**; b) J. W. Sekowski, L. H. Malkas, Y. Wei, R. J. Hickey, *Toxicol. Appl. Pharmacol.* **1997**, *145*, 268–276.
- [2] I. Onyido, A. R. Norris, E. Buncel, *Chem. Rev.* **2004**, *104*, 5911–5929.
- [3] S. Halbach, L. Kremers, H. Willruth, A. Mehl, G. Welzl, F. X. Wack, R. Hickel, H. Greim, *Hum. Exp. Toxicol.* **1997**, *16*, 667–672.
- [4] a) H. H. Harris, I. J. Pickering, G. N. George, *Science* **2003**, *301*, 1203–1203; b) S. Yoon, A. E. Albers, A. P. Wong, C. J. Chang, *J. Am. Chem. Soc.* **2005**, *127*, 16030–16031.
- [5] a) M. A. Nolan, S. P. Kounaves, *Anal. Chem.* **1999**, *71*, 3567–3573; b) S. P. Wang, E. S. Forzani, N. J. Tao, *Anal. Chem.* **2007**, *79*, 4427–4432.
- [6] a) E. M. Nolan, S. J. Lippard, *J. Am. Chem. Soc.* **2003**, *125*, 14270–14271; b) Y. K. Yang, K. J. Yook, J. Tae, *J. Am. Chem. Soc.* **2005**, *127*, 16760–16761; c) E. M. Nolan, S. J. Lippard, *J. Am. Chem. Soc.* **2007**, *129*, 5910–5918; d) M. K. Nazeeruddin, D. D. Censo, R. Humphry-Baker, M. Grätzel, *Adv. Funct. Mater.* **2006**, *16*, 189–194; e) S. Tatay, P. Gavina, E. Coronado, E. Palomares, *Org. Lett.* **2006**, *8*, 3857–3860.
- [7] P. Chen, C. He, *J. Am. Chem. Soc.* **2004**, *126*, 728–729.
- [8] a) I. B. Kim, U. H. F. Bunz, *J. Am. Chem. Soc.* **2006**, *128*, 2818–2819; b) Y. Tang, F. He, M. Yu, F. Feng, L. An, H. Sun, S. Wang, Y. Li, D. Zhu, *Macromol. Rapid Commun.* **2006**, *27*, 389–392.
- [9] a) H. Li, Y. Zhang, X. Wang, D. Xiong, Y. Bai, *Mater. Lett.* **2007**, *61*, 1474–1477; b) Z. X. Cai, H. Yang, Y. Zhang, X. P. Yan, *Anal. Chim. Acta* **2006**, *559*, 234–239; c) J. L. Chen, Y. C. Gao, Z. B. Xu, G. H. Wu, Y. C. Chen, C. Q. Zhu, *Anal. Chim. Acta* **2006**, *577*, 77–84.
- [10] a) R. M. Izatt, J. J. Christenson, J. H. Rytting, *Chem. Rev.* **1971**, *71*, 439–481; b) G. H. Clever, C. Kaul, T. Carell, *Angew. Chem.* **2007**, *119*, 6340–6350; *Angew. Chem. Int. Ed.* **2007**, *46*, 6226–6236.
- [11] a) T. Yamane, N. Davidson, *J. Am. Chem. Soc.* **1961**, *83*, 2599–2607; b) S. Mansy, R. S. Tobias, *Inorg. Chem.* **1975**, *14*, 287–291.
- [12] A. Ono, H. Togashi, *Angew. Chem.* **2004**, *116*, 4400–4402; *Angew. Chem. Int. Ed.* **2004**, *43*, 4300–4302.
- [13] X. Liu, Y. Tang, L. Wang, J. Zhang, S. Song, C. Fan, S. Wang, *Adv. Mater.* **2007**, *19*, 1471–1474.
- [14] J.-S. Lee, M. S. Han, C. A. Mirkin, *Angew. Chem.* **2007**, *119*, 4171–4174; *Angew. Chem. Int. Ed.* **2007**, *46*, 4093–4096.
- [15] J. Liu, Y. Lu, *Angew. Chem.* **2007**, *119*, 7731–7734; *Angew. Chem. Int. Ed.* **2007**, *46*, 7587–7590.
- [16] a) H. X. Li, L. Rothberg, *J. Am. Chem. Soc.* **2004**, *126*, 10958–10961; b) H. X. Li, L. Rothberg, *Anal. Chem.* **2004**, *76*, 5414–5417; c) L. Wang, X. Liu, X. Hu, S. Song, C. Fan, *Chem. Commun.* **2006**, 3780–3782.
- [17] H. X. Li, L. Rothberg, *Proc. Natl. Acad. Sci. USA* **2004**, *101*, 14036–14039.
- [18] H. Wei, B. Li, E. Wang, S. Dong, *Chem. Commun.* **2007**, 3735–3737.
- [19] C.-C. Huang, H.-T. Chang, *Chem. Commun.* **2007**, 1215–1217.
- [20] C.-C. Huang, Z. Yang, K.-H. Lee, H.-T. Chang, *Angew. Chem.* **2007**, *119*, 6948–6952; *Angew. Chem. Int. Ed.* **2007**, *46*, 6824–6828.
- [21] M. K. Beissenhirtz, I. Willner, *Org. Biomol. Chem.* **2006**, *4*, 3392–3401.
- [22] a) Y. Weizmann, M. K. Beissenhirtz, Z. Cheglakov, R. Nowarski, M. Kotler, I. Willner, *Angew. Chem.* **2006**, *118*, 7544–7548; *Angew. Chem. Int. Ed.* **2006**, *45*, 7384–7388; b) B. Shlyahovsky, D. Li, Y. Weizmann, R. Nowarski, M. Kotler, I. Willner, *J. Am. Chem. Soc.* **2007**, *129*, 3814–3815.
- [23] a) P. Travascio, Y. F. Li, D. Sen, *Chem. Biol.* **1998**, *5*, 505–517; b) P. Travascio, A. J. Bennet, D. Y. Wang, D. Sen, *Chem. Biol.* **1999**, *6*, 779–787.